# Dalton Transactions

Accepted Manuscript






ROYAL SOCIETY OF CHEMISTRY

www.rsc.org/dalton

# Chiral Transition–Metal Complexes as Brønsted–Acid Catalysts for the Asymmetric Friedel–Crafts Hydroxyalkylation of Indoles†

**Daniel Carmona,*[a] M. Pilar Lamata,[a] Antonio Sánchez,[a] Fernando Viguri,[a] Ricardo Rodríguez,[a] Luis A. Oro,[a] Chunhui Liu,[b] Silvia Díez–González,[b,c] and Feliu Maseras*[b,d]**

*Received …….*

*DOI: …….*

The Friedel–Crafts reaction between 3,3,3–trifluoropyruvates and indoles is efficiently catalysed by the iridium complex $[(\eta^5\text{–}C_5Me_5)Ir\{(R)\text{–Prophos}\}(H_2O)][SbF_6]_2$ (**1**) with up to 84% e.e. Experimental data and theoretical calculations support a mechanism involving the Brønsted–acid activation of the pyruvate carbonyl by the protons of the coordinated water molecule in **1**. Water is not dissociated during the process and, therefore, the catalytic reaction occurs with no direct interaction between the substrates and the metal.

[a] *Instituto de Síntesis Química y Catálisis Homogénea, Universidad de Zaragoza–Consejo Superior de Investigaciones Científicas, Pedro Cerbuna 12, 50009 Zaragoza, Spain*
[b] *Institute of Chemical Research of Catalonia (ICIQ), Av. Paisos Catalans 16, 43007 Tarragona, Spain*
[c] *Department of Chemistry, Imperial College London, Exhibition Road, South Kensington, London SW7 2Az, United Kingdom*
[d] *Departament de Química, Universitat Autònoma de Barcelona, 08193 Bellaterra, Spain*
*E-mail: dcarmona@unizar.es, fmaseras@iciq.es*

† Electronic supplementary information (ESI) available: Computational details, atomic coordinates and absolute energies of computed structures. See DOI:

## Introduction

Chiral Brønsted–acid catalysis is a rapidly growing area of organocatalysis.[1] As the most representative examples, enantioselective catalytic systems based on (thio)ureas[1d-g,m-o,r,x] diols,[1e,g,j,m,x] or phosphoric acids[1e,h,j,l,m,q,u-x] have been recently employed for the activation of electrophiles towards nucleophilic attack. The H–bond donating ability of the catalysts is usually increased by means of electron–withdrawing substituents. However, metal containing substituents have been rarely employed to this end. In this respect, Yamamoto *et al*. reported that coordination of binols[2a-c] or an hydroxyl-phosphane ligand derived from binol[2d] to $SnCl_4$ or to La(OTf), respectively, enhances the acidity of the OH groups, rendering active Brønsted–acid catalysts for the enantioselective protonation of silyl enol ethers and biomimetic cyclization of polyprenoid. Furthermore, Toste et al. have successfully applied to the former process, chiral Brønsted–acids derived from the activation of the OH group of EtOH or *i*PrOH by coordination to gold diphosphane complexes.[3] On the other hand, the collaboration of a water ligand in the redox isomerisation of allylic alcohols in aqueous medium by Ru(IV) based complexes has been recently reported.[4]

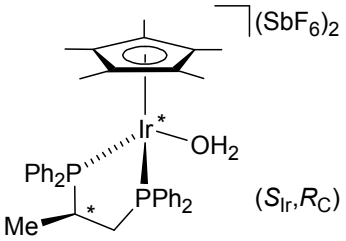


**1**

**Scheme 1** Brønsted–acid catalyst **1**

In this line, in the present communication we disclose the use of the water adduct of the chiral iridium fragment ($\eta^5$–$C_5Me_5$)Ir{(*R*)–Prophos} (Prophos = propane–1,2–diylbis(diphenylphosphane)[5] (**1**) as chiral Brønsted–acid catalyst, through its coordinated water molecule (Scheme 1). Water is one of the simplest molecules with

Brønsted–acid capabilities. The coordination of water molecules to the carbonyl function in Diels–Alder reactions[6] and Claisen rearrangements,[7] resulted in rate enhancements and the manifold role of water in some organocatalytic reactions has been extensively discussed.[8] However, as far as we know, the direct involvement of a water molecule in chiral metal–containing Brønsted–acid catalysis has been rarely reported so far.[2,3]

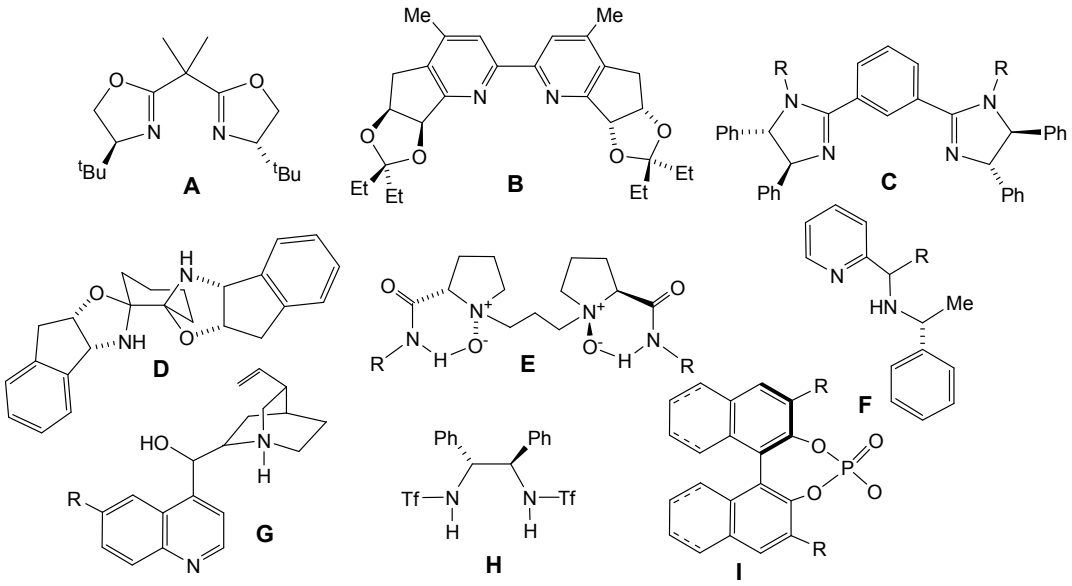


**Scheme 2** Chiral ligands/catalysts employed in hydroxyalkylation of indoles

On the other hand, the Friedel–Crafts (FC) reaction is a powerful strategy for the alkylation of aromatic and heteroaromatic substrates and constitutes an important reaction for the formation of C–C bonds.[9] Asymmetric protocols for both metal– and organo–catalysed FC reactions have been reported.[10] In particular, enantioselective hydroxyalkylation of indoles with 3,3,3–trifluoropyruvates has been achieved using copper(II)–, zinc(II)– or ytterbium(III) based chiral Lewis acids with bisoxazoline (**A**),[11] 2,2'–bipyridyl (**B**),[12] bis(imidazoline) (**C**)[13] or bisoxazolidine (**D**),[14] N,N'–dioxide (**E**),[15] or pyridylamine (**F**)[16] ligands, as well as, using cinchona alkaloids (**G**),[17] bis(sulfonamides) (**H**),[18] or chiral phosphoric acids (**I**)[19] as organocatalysts (Scheme 2).

Recently, Rueping et al. have reported the application of calcium phosphates to this reaction.[20]

In the present paper we report our results on the hydroxyalkylation of indoles with 3,3,3–trifluoropyruvates using complex **1** as catalyst.

**Results and Discussion**

When, at –78 ºC, one equivalent of ethyl 3,3,3–trifluoropyruvate **2a** was added to a $CD_2Cl_2$ solution of **1**, in the presence of 4Å MS,[21] no significant changes were observed in the $^{1}H$, $^{13}C$, $^{31}P$ and $^{19}F$ NMR spectra of the resulting solution, with respect to those of the starting materials. However, the subsequent addition of one equivalent of indole **3a** produced instantaneously the quantitative formation of the alkylation Friedel–Crafts product (*S*)–**4a**, in 71% enantiomeric excess[11,13] (Scheme 3).

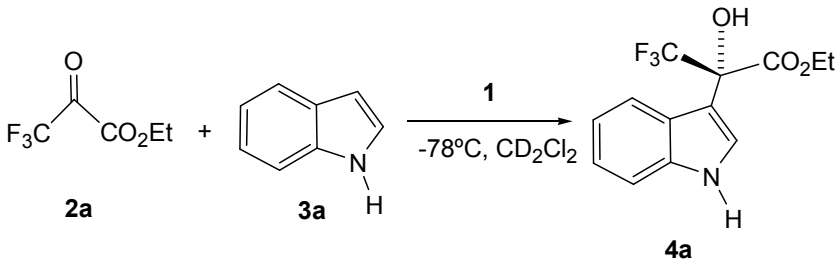


**Scheme 3** Catalytic FC reaction

As the sole possible source of chirality is compound **1**, we looked for interactions between **1** and the organic substrates. In this regard, we observed that successive addition of **2a** to a $CD_2Cl_2$ solution of **1**, at -25 ºC, in the presence of 4Å MS, produced, as the unique significant NMR change, a gradual displacement of the chemical shift of the water protons from 2.56 (δ value in the absence of **2a**) to 2.87 ppm (30 equiv. of **2a** added, Scheme 4). In an independent experiment, addition of indole **3a** (up to 5 equiv.) to $CD_2Cl_2$ solutions of **1** did not alter significantly the NMR spectra. These data suggest

that complex **1** catalyzes the FC reaction acting as a Brønsted–acid catalyst through its coordinated water molecule.

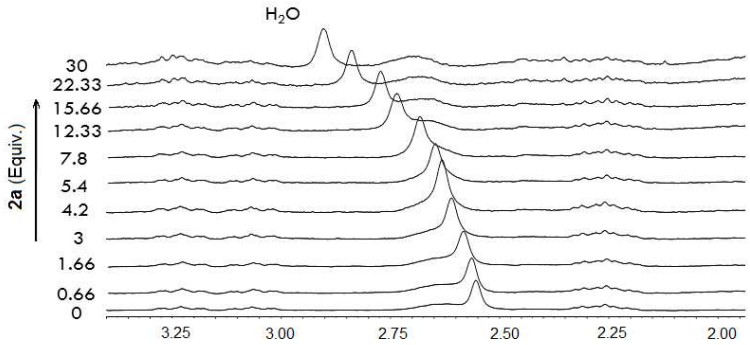


**Scheme 4** Shift of the $^{1}$H NMR signal of the water protons in **1** after addition of **2a**

This hypothesis was confirmed by a series of DFT calculations of the reaction mechanism on the model system defined by ($\eta^5$–$C_5H_5$)Ir($H_2PCH_2CH_2PH_2$)($H_2O$) (**1–t**), methyl 3,3,3–trifluoropyruvate (**2a–t**) and indole (**3a**). Structures were optimized and free energies in solution are reported in what follows. The key structures in the reaction

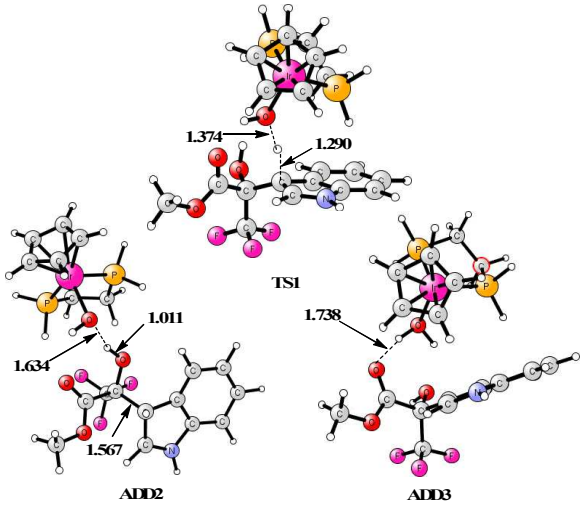


**Figure 1** M06 optimized structures of adducts **ADD2**, **ADD3**, and of transition state **TS1**. Selected distances are given in Å.

profile are presented in Figure 1. The calculation in the potential energy surface of the sequential approach between the reacting fragments produces two stable adducts that disappear as such when free energy corrections are introduced. They are however informative on the reaction pathway. The initial approach between the metal complex

**1–t** and the pyruvate **2a–t** produces an adduct **ADD1** (not shown), containing a hydrogen bond, has a free energy of 9.2 kcal.mol$^{-1}$ above the separate reactants. The approach of indole **3a** to **ADD1** results in the barrierless formation of species **ADD2**, with a relative free energy of 17.7 kcal.mol$^{-1}$. In **ADD2** (see Figure 1), the new carbon–carbon bond is already formed (1.567 Å), and a hydrogen is transferred from the water molecule (O–H, 1.634 Å) to a carbonyl of the pyruvate (O–H, 1.011 Å). **ADD2** is an ion pair between an anionic metal complex and the protonated product. The reaction continues through transition state **TS1**. In **TS1** (see Figure 1) a hydrogen atom is transferred from the indole (C–H 1.290 Å) back to the metal complex (O–H 1.374 Å). **TS1** is 20.4 kcal.mol$^{-1}$ above the separate reactants. This is the highest free energy in the whole process and is consistent with the experimental observation of a fast process. **TS1** evolves towards **ADD3** (Figure 1), where the Friedel–Crafts product is weakly bound to the catalyst through a hydrogen bond. **ADD3** is 0.7 kcal.mol$^{-1}$ above the separate reactants. Separation of the product and regeneration of the **1–t** catalyst is favorable in the free energy scale, the overall exoergodicity of the whole process is –12.4 kcal mol$^{-1}$. Other reaction pathways may be envisaged. On one hand, there is a certain margin for conformational diversity in this model system, but we decided to analyze it on the study on enantioselectivity in the real system that follow below. Other pathways involving direct coordination of lone pairs in the reactants to the iridium center in **1-t** are not feasible because of the 18–electron nature of the metal complex.

The full computed free energy profile for the model system is presented in Figure 2. It is worth noticing that most of the free energy cost is associated to the entropically disfavored process of bringing the three fragments together (catalyst plus two substrates), as the adduct **ADD2** is already 17.7 kcal.mol$^{-1}$ above the separate reactants. The key transition state **TS1** is only 3.2 kcal.mol$^{-1}$, thus accounting for the fast reaction.

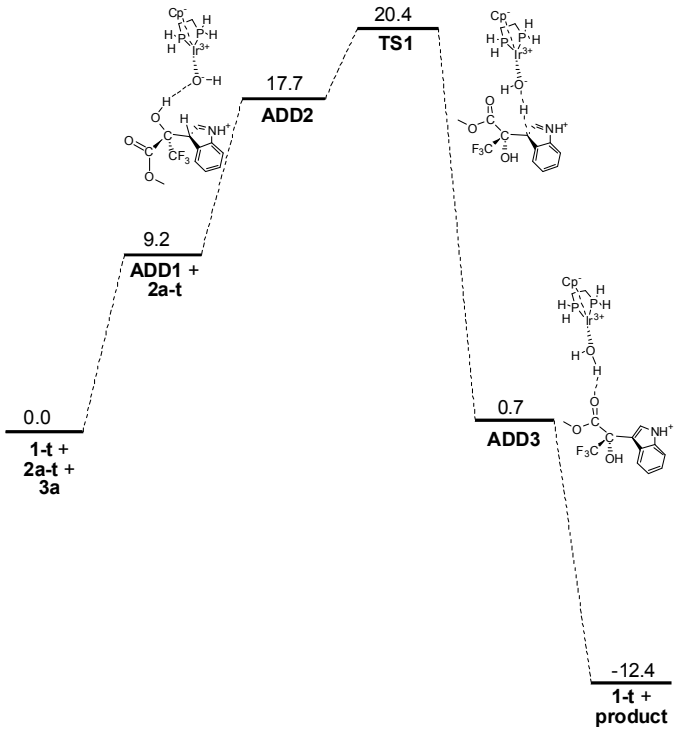


**Figure 2**. Computed free energy profile (kcal.mol$^{-1}$) for the reaction in the model system.

The catalytic role of the metal complex seems to be the modulation of the acid/base properties of the coordinated water. This water has to be acidic enough to transfer a proton to the pyruvate–indole pair, but the resulting hydroxyl group has to be basic enough to deprotonate the resulting intermediate. Similar electronic balances seem to be at play in the substrates. Most probably, the presence of the two electron–withdrawing groups, $CF_3$ and $CO_2Et$, on the pyruvate carbonyl, precludes direct pyruvate coordination to the metal accompanied by water substitution. However, the carbonyl pyruvate group is nucleophilic enough to establish hydrogen–bonding interactions with one of the water protons, becoming activated for the nucleophilic attack of the indole.

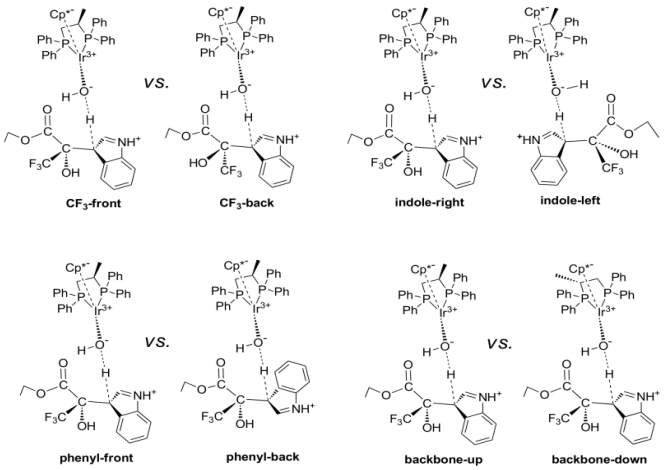


**Figure 3** Four conformational dichotomies in the definition of the structure for transition state **TS1–full** in real system.

We tackled next the problem of enantioselectivity from a computational point of view. This required the introduction of the full experimental system, as the model system discussed above is too simplified. In this concern, the results from calculations on model system are still significant because they indicate it is possible to concentrate on the energy of **TS1**, which is the highest energy point in the free energy profile.[22] The introduction of the real substituent in **TS1** creates a variety of possible conformations, which have to be analyzed.[23] We can classify the conformations according to the four structural dichotomies described in Figure 3. The structure of **TS1** (Figure 1) is such that the ester substituent in the newly created stereogenic center is acting as acceptor of a weak hydrogen bond from the hydroxyl group bound to the metal, and as such its position is fixed in that direction. As a result, the trifluoromethyl group can point either to the front (**$CF_3$–front**) or to the back (**$CF_3$–back**) in the representation described in Figure 3. In this same representation, the indole group can be placed to the right (**indole–right**) or to the left (**indole–left**) of this stereogenic carbon. Of course, the combination of the position of $CF_3$ and indole will define the stereochemistry (*R* or *S*) of the newly formed stereocenter. There are however two other sources of conformational complexity that must be taken into account: the position of the phenyl part of the indole

(**phenyl–front** or **phenyl–back**), and the arrangement of the diphosphane backbone (**backbone–up** or **backbone–down**). The combination of the four dichotomies results in 16 possible conformations of this transition state, which were optimized. Their relative energies are summarized in Table 1. There are also other conformational complexities associated to the arrangement of the phenyl groups (edge or face) with respect to the Ir–P bonds, or to the involvement of the other hydrogen of water in the network of hydrogen bonds. They were also analyzed, and the results presented here correspond only to the most stable arrangement in each case.

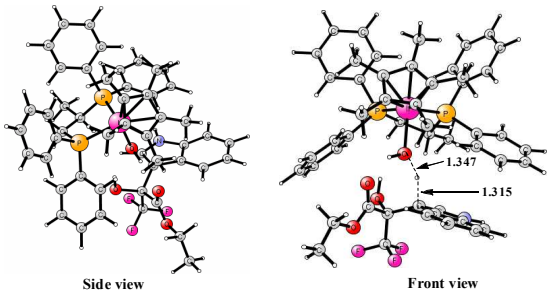


**Figure 4** Two views of the optimized structure of transition state **STS1–2full**.

The relative energies in Table 1 are given with respect to the most stable conformation of the transition state, **STS1–2full**. We can use the five most stable conformers, which are those within 3.0 kcal $mol^{-1}$ of the most stable one, to obtain a computed enantiomeric excess at the experimental temperature of –78 ºC. This results in a value of 81% e.e. in favor of the *S* enantiomer. The proper product is predicted, and the computed enantiomeric excess is close to the experimental result of 71 % e.e. The visual analysis of the computed structures is not trivial, as seen from the structure of the most stable conformer **STS1–2full**, shown in Figure 4. It is however clear that it

**Table 1** Computed relative free energies (kcal $mol^{-1}$) in solution and conformational Identity of the different forms of TS1

| Label | Energy | $CF_3$ | Indole | Phenyl | Backbone |
|---|---|---|---|---|---|
| **RTS1–1full** | 5.1 | Back | Right | Back | Up |
| **RTS1–2full** | 8.8 | Back | Right | Front | Up |

| | | | | | |
|---|---|---|---|---|---|
| **RTS1–3full** | 5.0 | Front | Left | Back | Up |
| **RTS1–4full** | 0.8 | Front | Left | Front | Up |
| **RTS1–5full** | 10.3 | Back | Right | Back | Down |
| **RTS1–6full** | 4.3 | Back | Right | Front | Down |
| **RTS1–7full** | 6.9 | Front | Left | Back | Down |
| **RTS1–8full** | 2.6 | Front | Left | Front | Down |
| **STS1–1full** | 0.5 | Front | Right | Back | Up |
| **STS1–2full** | 0.0 | Front | Right | Front | Up |
| **STS1–3full** | 6.9 | Back | Left | Back | Up |
| **STS1–4full** | 5.1 | Back | Left | Front | Up |
| **STS1–5full** | 6.3 | Front | Right | Back | Down |
| **STS1–6full** | 1.5 | Front | Right | Front | Down |
| **STS1–7full** | 7.1 | Back | Left | Back | Down |
| **STS1–8full** | 5.9 | Back | Left | Front | Down |

corresponds to the same transition state computed for the model system with the hydrogen transfer from the indole (C–H 1.315 Å) to the metal complex (O–H 1.347 Å). The qualitative analysis of the nature of the most stable conformers is informative. In four of the five most stable conformers, both $CF_3$ and phenyl are in the front arrangement. This means that they point away from the phosphane, and fits well with the intuitive view that $CF_3$ and phenyl are the bulkier substituents at the piruvate and indole moieties, respectively; and that the phosphane side is more sterically hindered than the cyclopentadienyl side in the iridium complex. It must be also noticed that the most stable conformations going to the *S* product (**STS1–2full**) and to the *R* product (**RTS1–4full**) agree in all the conformational labels but in the indole orientation, which is right for the *S* isomer, and left for the *R* isomer. This indicates that the $CF_3$ is more sterically active, and that the right side of the molecule (in the orientation in Figure 3) is the most sterically hindered. This correlates well with the presence of the extra methyl substituent in the diphosphane in this right–hand side, which brings more steric pressure to this part of the system. Therefore the combination of electronic and steric effects places the substituents at the new stereogenic center being formed in a particular arrangement, deciding the configuration of the product, in a form reminiscent of what happens in asymmetric hydrogenation.[24] For our particular reaction, there are a variety

of interactions involved, the energy effect of each of them is relatively small, and the system remains quite flexible, and because of this the enantiomeric excess is limited.

Next, reactions of **2a** or its methyl analogue 3,3,3–trifluoropyruvate **2b** with various indoles (**3**) were performed in a substoichiometric manner (Table 2). Typically, at –70 ºC, with a catalytic loading of 5 mol %, reactions reached completion within 15 min. Moderate to good e.e.'s were achieved in all cases. The catalyst tolerates both electron–donating (entries 5, 7) and withdrawing (entries 6, 8) substituents at the 5 position of the indole, without e.e. erosion. On the contrary, in general, this substitution slightly increases the e.e.. *N*–Methylation lowers the chiral induction (compare entries 1

**Table 2** Asymmetric FC hydroxyalkylation reactions of indoles with pyruvates

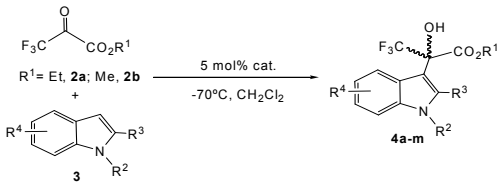


| Entry | Cat. | $R^1$ | $R^2$ | $R^3$ | $R^4$ | t (min) | Product | Yield (%)[a] | e.e. (%)[b] |
|---|---|---|---|---|---|---|---|---|---|
| **1** | **1** | Et | H | H | H | 20 | **4a** | >99 | 65 |
| **2** | **1** | Et | Me | H | H | 20 | **4b** | >99 | 47 |
| **3** | **1** | Et | H | Me | H | 25 | **4c** | >99 | 76 |
| **4** | **1** | Et | Me | Me | H | 20 | **4d** | 96 | 52 |
| **5** | **1** | Et | H | H | 5–OMe | 20 | **4e** | >99 | 71 |
| **6** | **1** | Et | H | H | 5–Cl | 15 | **4f** | 96 | 76 |
| **7** | **1** | Et | H | Me | 5–OMe | 14 | **4g** | 97 | 55 |
| **8** | **1** | Et | H | Me | 5–Cl | 15 | **4h** | >99 | 80 |
| **9** | **1** | Me | H | H | H | 15 | **4i** | >99 | 68 |
| **10** | **1** | Me | Me | H | H | 15 | **4j** | 98 | 50 |
| **11** | **1** | Me | H | Me | H | 14 | **4k** | 99 | 71 |
| **12** | **1** | Me | H | H | 5–Cl | 14 | **4l** | 95 | 80 |
| **13** | **1** | Me | H | Me | 5–Cl | 14 | **4m** | 99 | 84 |
| **14**[c] | **1** | Et | H | Me | 5–Cl | 15 | **4h** | 99 | 73 |
| **15**[d] | **1** | Et | H | Me | 5–Cl | 15 | **4h** | 99 | 72 |
| **16** | **5** | Et | H | Me | H | 15 | **4c** | 99 | 69 |
| **17** | **5** | Et | H | Me | 5–Cl | 15 | **4h** | 98 | 71 |
| **18** | **5** | Me | H | Me | H | 15 | **4k** | >99 | 73 |
| **19** | **5** | Me | H | Me | 5–Cl | 15 | **4m** | 99 | 83 |
| **20** | **6** | Et | H | Me | 5–Cl | 15 | **4h** | 92 | 8 |
| **21** | **7** | Et | H | Me | 5–Cl | 15 | **4h** | 99 | 34 |

Reaction conditions: catalyst 0.03 mmol (5.0 mol %), pyruvate 0.90 mmol, 100 mg of 4 Å molecular sieves, and indole 0.60 mmol in 4 mL of $CH_2Cl_2$. [a] Based on indole. Determined by NMR. [b] Determined by HPLC. [c] Catalyst loading 2 mol %. [d] Catalyst loading 1 mol %.

with 2, 3 with 4, or 9 with 10), but not as dramatically as in previously reported examples,[12,13,17a] confirming that, in our system, the NH functionality does not play a relevant role in the hydroxyalkylation mechanism. When the reaction was carried out with only 2 or 1 mol % of **1**, quantitative yields were also achieved in 15 min, with moderate losses in the e.e. values (entries 14 and 15 versus entry 8). Thus, TOF's of about 400 $h^{-1}$ at complete conversion were achieved, the highest reported so far for this kind of FC transformation.[11-20] Notably, the homologous rhodium complex[25] ($S_{Rh}$,$R_C$)–[($\eta^5$–$C_5Me_5$)Rh{(*R*)–Prophos}($H_2O$)][$SbF_6$]$_2$ (**5**) is also an efficient catalyst for the process that affords similar selectivity (entries 16–19). Related half–sandwich ruthenium, ($S_{Ru}$,$R_C$)–[($\eta^6$–*p*–$MeC_6H_4$*i*Pr)Ru{(*R*)–Prophos}($H_2O$)][$SbF_6$]$_2$ (**6**), and osmium complexes, [($S_{Os}$,$R_C$) and ($R_{Os}$,$R_C$)]–[($\eta^6$–*p*–$MeC_6H_4$*i*Pr)Os{(*R*)–Prophos}($H_2O$)][$SbF_6$]$_2$ (**7**, 87/13:($S_{Os}$,$R_C$)/($R_{Os}$,$R_C$) mixture),[26] also actively catalyse the FC reaction but with poorer e.e.'s (entries 20–21).

## Conclusions

In summary, in this paper we report on the use of a water adduct of a dicationic chiral iridium Lewis–acid for the enantioselective FC hydroxyalkylation of indoles with 3,3,3–trifluoropyruvates. The whole complex acts as a Brønsted–acid catalyst through the protons of the coordinated water molecule. The function of the metal moiety is twofold: as a Lewis acid, it enhances the acidity of the water protons and, as a chiral fragment, it governs the stereochemistry of the process. The findings reported herein may contribute to the development of a new metal–containing Brønsted–acid catalyst type in which the Brønsted acidity relies on an M–XH (M = metal, X = O, N, S) functionality and the stereoelectronic control is provided by the metallic moieties. Further studies to establish the scope of this methodology are in progress.

## Experimental

### General information

All solvents were treated in a PS-400-6 Innovative Technolog Solvent Purification System (SPS), and degassed prior to use. All preparations were carried out under argon. $^{1}H$, $^{13}C$, $^{31}P$, and $^{19}F$ NMR spectra were recorded on Bruker AV-300, Bruker AV-400 or Bruker AV-500 spectrometers. Chemical shifts are expressed in ppm upfield from $SiMe_4$ ($^{1}H$ and $^{13}C$), 85% $H_3PO_4$ ($^{31}P$) or $CFCl_3$ ($^{19}F$). Analytical high performance liquid chromatography (HPLC) was performed on an Alliance Waters (Water 2996 PDA detector) instrument using a chiral column Daicel Chiralcel OD-H (0.46 cm × 25 cm) with OD-H guard (0.46 × 5 cm).

### Catalytic experimental procedure

Under argon, in a Schlenk flask equipped with a magnetic stirrer, the corresponding metal complex (0.03 mmol) was dissolved in $CH_2Cl_2$ (4 mL), at –70 ºC. The mixture was stirred for 10 minutes and then 4 Å Molecular Sieves (100 mg) was added. After stirring for another 10 minutes, the corresponding 3,3,3–trifluoropyruvate (0.90 mmol) and indole (0.60 mmol) were added. After the appropriate reaction time, the process was quenched by addition of 2 mL of methanol. The solution was concentrated under vacuum to dryness and the residue was extracted with 2 × 10 mL of diethyl ether. The resulting suspension was filtered over Celite and evaporated to dryness. The pale yellow oil or white solid obtained was analyzed and characterized by NMR and HPLC techniques.

### Ethyl 3,3,3-trifluoro-2-hydroxy-2-(indol-3-yl)propionate (4a)[11,13]

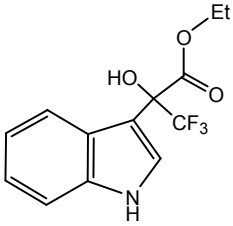


$^{1}H$ NMR 500.13 MHz ($CDCl_3$): $\delta$ 1.38 (t, $J$ = 7.1 Hz, 3H, $CH_3$), 4.35-4.52 (m, 2H, $CH_2$), 4.40 (s, 1H, OH), 7.18 (t,

*J* = 7.6 Hz, 1H, Ar), 7.26 (t, *J* = 7.6 Hz, 1H, Ar), 7.41 (d, *J* = 8.3 Hz, 1H, Ar), 7.51 (br d, 1H, Ar), 7.93 (d, 1H, Ar), 8.32 (br s, 1H, NH). $^{19}$F NMR 282 MHz ($CDCl_3$): $\delta$ -75.1 (s). HPLC (Daicel Chiralcel OD-H with OD-H guard, *n*-hexane/*i*PrOH (90/10), 1 mL/min) $t_R$ 12.7 (*S*) and 16.3 (*R*) min (minor).

**Ethyl 3,3,3-trifluoro-2-hydroxy-2-(*N*-methyl-indol-3-yl)propionate (4b)**[13,18]

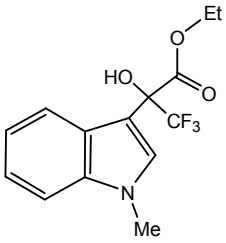


$^1$H NMR 300.13 MHz ($CDCl_3$): $\delta$ 1.36 (t, *J* = 7.2 Hz, 3H, $CH_3$), 3.79 (s, 3H, $CH_3$), 4.33-4.50 (m, 2H, $CH_2$), 4.38 (s, 1H, OH), 7.14-7.34 (m, 4H, Ar), 7.90 (d, *J* = 8.2 Hz, 1H, Ar). $^{19}$F NMR 282 MHz ($CDCl_3$): $\delta$ -76.8 (s). HPLC (Daicel Chiralcel OD-H with OD-H guard, *n*-hexane/*i*PrOH (90/10), 1 mL/min) $t_R$ 11.84 (*S*) and 21.37 (*R*) min (minor).

**Ethyl 3,3,3-trifluoro-2-hydroxy-2-(2-methyl-indol-3-yl)propionate (4c)**[13]

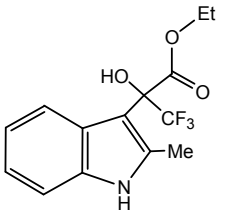


$^1$H NMR 300.13 MHz ($CDCl_3$): $\delta$ 1.37 (t, *J* = 7.2 Hz, 3H, $CH_3$), 2.53 (s, 3H, $CH_3$), 4.32-4.52 (m, 2H, $CH_2$), 4.01 (s, 1H, OH), 7.08-7.29 (m, 3H, Ar), 7.83 (d, *J* = 8.19 Hz, 1H, Ar), 8.01 (br s, 1H, NH). $^{19}$F NMR 282 MHz ($CDCl_3$): $\delta$ -75.1 (s). HPLC (Daicel Chiralcel OD-H with OD-H guard, *n*-hexane/*i*PrOH (90/10), 1 mL/min) $t_R$ 13.4 (*S*) (minor) and 17.9 (*R*) min.

**Ethyl 3,3,3-trifluoro-2-hydroxy-2-(*N*-methyl-2-methyl-indol-3-yl)propionate (4d)**[11]

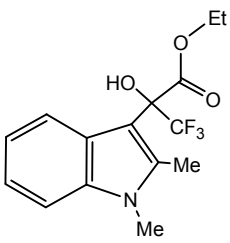


$^1$H NMR 300.13 MHz ($CDCl_3$): $\delta$ 1.37 (t, *J* = 6.7 Hz, 3H, $CH_3$), 2.56 (s, 3H, $CH_3$), 3.68 (s, 3H, $NCH_3$), 4.33-4.50 (m, 2H, $CH_2$), 3.82 (s, 1H, OH), 7.09-7.30 (m, 3H, Ar), 7.82 (d, *J* = 7.7 Hz, 1H, Ar). $^{19}$F NMR 282 MHz ($CDCl_3$): $\delta$ -75.8 (s). HPLC (Daicel Chiralcel OD-H with OD-H guard, *n*-hexane/*i*PrOH (90/10), 1 mL/min) $t_R$ 9.13 (*S*) (minor) and 10.61 (*R*) min.

**Ethyl 3,3,3-trifluoro-2-hydroxy-2-(5-methoxy-indol-3-yl)propionate (4e)**[13]

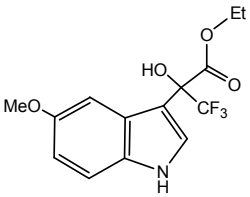

$^1$H NMR 300.13 MHz ($CDCl_3$): $\delta$ 1.35 (t, $J$ = 6.7 Hz, 3H, $CH_3$), 3.86 (s, 3H, $OCH_3$), 4.28-4.59 (m, 2H, $CH_2$), 4.33 (s, 1H, OH), 6.88-6.91 (m, 1H, Ar), 7.18-7.21 (m, 1H, Ar), 7.33-7.44 (m, 2H, Ar), 8.34 (br s, 1H, NH). $^{19}$F NMR 282 MHz ($CDCl_3$) $\delta$ -76.6 (s). HPLC (Daicel Chiralcel OD-H with OD-H guard, *n*-hexane/*i*PrOH (90/10), 1 mL/min) $t_R$ 17.8 (*S*) and 25.7 (*R*) min (minor).

**Ethyl 3,3,3-trifluoro-2-hydroxy-2-(5-chloro-indol-3-yl)propionate (4f)**[13]

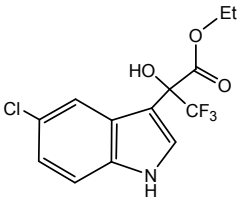

$^1$H NMR 300.13 MHz ($CDCl_3$): $\delta$ 1.39 (t, $J$ = 6.7 Hz, 3H, $CH_3$), 4.35-4.54 (m, 2H, $CH_2$), 4.41 (s, 1H, OH), 7.18-7.32 (m, 2H, Ar), 7.53 (d, $J$ = 2.8 Hz 1H, Ar), 7.95 (s, 1H, Ar), 8.33 (br s, 1H, NH). $^{19}$F NMR 282 MHz ($CDCl_3$): $\delta$ -77.1 (s). HPLC (Daicel Chiralcel OD-H with OD-H guard, *n*-hexane/*i*PrOH (90/10), 1 mL/min) $t_R$ 26.3 (*S*) and 34.6 (*R*) min (minor).

**Ethyl 3,3,3-trifluoro-2-hydroxy-2-(5-methoxy-2-methyl-indol-3-yl)propionate (4g)**

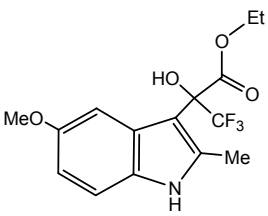

$^1$H NMR 300.13 MHz ($CDCl_3$): $\delta$ 1.37 (t, $J$ = 7.2 Hz, 3H, $CH_3$), 2.51 (s, 3H, $CH_3$), 3.85 (s, 3H, $OCH_3$), 3.94 (s, 1H, OH), 4.31-4.52 (m, 2H, $CH_2$), 6.82 (dd, $J$ = 8.7, 2.6 Hz 1H, Ar), 7.16 (d, 1H, Ar), 7.33 (br s, 1H, Ar), 7.93 (br s, 1H, NH). $^{19}$F NMR 282 MHz ($CDCl_3$): $\delta$ -77.0 (s). ). $^{13}$C NMR 125 MHz ($CDCl_3$): δ 13.9, 14.3, 55.9, 63.5, 103.0, 103,8, 110.8, 111.6, 122.8, 125.11, 127.4, 129.7, 135.7, 154.3, 169.3. HPLC (Daicel Chiralcel OD-H with OD-H guard, *n*-hexane/*i*PrOH (90/10), 1 mL/min) $t_R$ 19.2 (minor) and 32.9 min.

**Ethyl 3,3,3-trifluoro-2-hydroxy-2-(5-chloro-2-methyl-indol-3-yl)propionate (4h)**

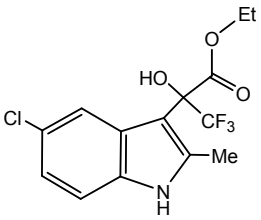


$^1$H NMR 300.13 MHz ($CDCl_3$): $\delta$ 1.42 (t, $J$ = 6.7 Hz, 3H, $CH_3$), 2.56 (s, 3H, $CH_3$), 4.36-4.54 (m, 2H, $CH_2$), 4.05 (s, 1H, OH), 7.10 (d, $J$ = 8.6, 1H, Ar), 7.18 (d, $J$ = 8.6, 1H, Ar), 7.86 (s, 1H, Ar), 8.03 (br s, 1H, NH). $^{19}$F NMR 282 MHz ($CDCl_3$): $\delta$ -76.3 (s). $^{13}$C NMR 125 MHz ($CDCl_3$): δ 13.9, 14.5, 64.0, 103.7, 111.2, 120.4, 121.9, 122.6, 124.9, 126.0, 127.8, 133.0, 136.9, 169.2. HPLC (Daicel Chiralcel OD-H with OD-H guard, *n*-hexane/*i*PrOH (90/10), 1 mL/min) $t_R$ 11.3 (minor) and 16.0 min.

**Methyl 3,3,3-trifluoro-2-hydroxy-2-(indol-3-yl)propionate (4i)**[12]

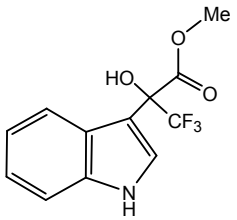


$^1$H NMR 300.13 MHz ($CDCl_3$): $\delta$ 3.96 (s, 3H, $CH_3$), 4.37 (s, 1H, OH), 7.16-7.28 (m, 2H, Ar), 7.39(d, $J$ = 7.7 Hz, 1H, Ar), 7.47 (d, $J$ =2.1 Hz, 1H, Ar), 7.88 (d, $J$ =8.2 Hz, 1H, Ar), 8.29 (br s, 1H, NH). $^{19}$F NMR 282 MHz ($CDCl_3$): $\delta$ -75.2 (s). HPLC (Daicel Chiralcel OD-H with OD-H guard, *n*-hexane/*i*PrOH (90/10), 1 mL/min) $t_R$ 16.7 and 19.2 min (minor).

**Methyl 3,3,3-trifluoro-2-hydroxy-2-(*N*-methyl-indol-3-yl)propionate (4j)**[12]

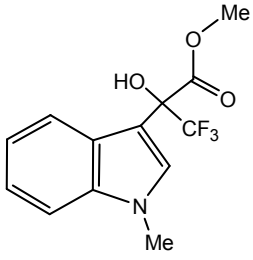


$^1$H NMR 300.13 MHz ($CDCl_3$): $\delta$ 3.81 (s, 3H, $NCH_3$), 3.96 (s, 3H, $CH_3$), 4.32 (s, 1H, OH), 7.15-7.36 (m, 4H, Ar), 7.86 (d, $J$ = 8.2 Hz, 1H, Ar). $^{19}$F NMR 282 MHz ($CDCl_3$): $\delta$ -76.7 (s). HPLC (Daicel Chiralcel OD-H with OD-H guard, *n*-hexane/*i*PrOH (90/10), 1 mL/min) $t_R$ 10.8 and 15.9 min (minor).

**Methyl 3,3,3-trifluoro-2-hydroxy-2-(2-methyl-indol-3-yl)propionate (4k)**[12]

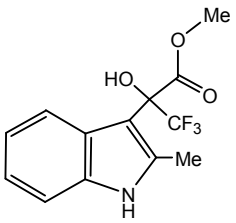

$^1$H NMR 300.13 MHz ($CDCl_3$): $\delta$ 2.49 (s, 3H, $CH_3$), 3.94 (s, 3H, $CH_3$), 3.97 (s, 1H, OH), 7.11-7.27 (m, 3H, Ar), 7.78 (d, $J$ =7.7 Hz, 1H, Ar), 8.02 (br s, 1H, NH). $^{19}$F NMR 282 MHz ($CDCl_3$): $\delta$ -77.3 (s). HPLC (Daicel Chiralcel OD-H with OD-H guard, *n*-hexane/*i*PrOH (90/10), 1 mL/min) $t_R$ 17.37 (minor) and 26.0 min.

**Methyl 3,3,3-trifluoro-2-hydroxy-2-(5-chloro-indol-3-yl)propionate (4l)**[19a]

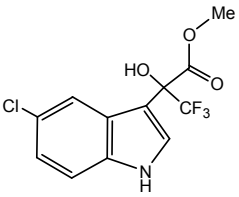

$^1$H NMR 300.13 MHz ($CDCl_3$): $\delta$ 3.97 (s, 3H, $CH_3$), 4.39 (s, 1H, OH), 7.19 (dd, $J$ = 8.7, 2.0 Hz, 1H, Ar), 7.29 (d, $J$ = 8.7 Hz, 1H, Ar), 7.49 (d, $J$ = 2.0 Hz, 1H, Ar), 7.89 (br d, 1H, Ar), 8.45 (br s, 1H, NH). $^{19}$F NMR 282 MHz ($CDCl_3$): $\delta$ -77.0 (s). HPLC (Daicel Chiralcel OD-H with OD-H guard, *n*-hexane/*i*PrOH (95/5), 1 mL/min) $t_R$ 39.9 and 43.8 min (minor).

**Methyl 3,3,3-trifluoro-2-hydroxy-2-(5-chloro-2-methyl-indol-3-yl)propionate (4m)**

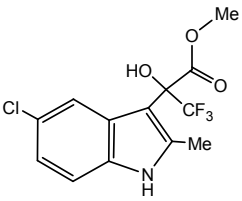

$^1$H NMR 300.13 MHz ($CDCl_3$): $\delta$ 2.52 (s, 3H, $CH_3$), 3.97 (s, 3H, $CH_3$), 3.99 (s, 1H, OH), 7.13 (d, $J$ = 8.6, 1H, Ar), 7.20 (d, $J$ = 8.6, 1H, Ar), 7.79 (s, 1H, Ar), 8.07 (br s, 1H, NH). $^{19}$F NMR 282 MHz ($CDCl_3$): δ -77.5 (s). $^{13}$C NMR 125 MHz ($CDCl_3$): $\delta$ 14.2, 53.9, 103.8, 111.2, 120.0, 122.0, 122.6, 124.8, 126.2, 127.9, 133.0, 136.6, 169.6. HPLC (Daicel Chiralcel OD-H with OD-H guard, *n*-hexane/*i*PrOH (90/10), 1 mL/min) $t_R$ 13.1 (minor) and 19.6 min.

**Computational Details**

Density functional theory (DFT) calculations were performed using the Gaussian09 suite of programs[27] with the M06 functional.[28] The structures were optimized using the

SDD basis set[29] for Ir, while the 6–31G(d)[30] basis set was used for all remaining atoms C, O, P, N, F, and H. The geometries were optimized without symmetry constraints. The nature of the stationary points as minima or transition states was confirmed by frequency calculations. The connectivity between the transition state and the associated minima was confirmed by a combination of intrinsic reaction coordinate (IRC) calculations (in the region near the transition state) and geometry optimization (connecting the final point of the IRC to the local minimum). Solvation effects were introduced through single-point calculations based on the gas phase structures with SMD mode[31] (SMD, ε= 8.93 for dichloromethane) at the M06 level using the SDD basis set for Ir, while the 6–31+G (d) basis set for all remaining atoms. The potential energies in solution were taken directly from the SCRF calculation, and the free energies in solution were obtained from the additional introduction of gas phase free energy corrections. The temperature used in these frequency calculations was the experimental value of -78 ºC, and the pressure was 1 atm. All reported energy values in the text are free energies in solution unless otherwise stated.

**Acknowledgements**

The authors acknowledge the Ministerio de Economía y Competitividad (MINECO, Grants CTQ2006–03030/BQU, CTQ2009–10303/BQU, CTQ2011–27033 and Consolider Ingenio 2010 CSD2006–003), Gobierno de Aragón (Grupo Consolidado: Catálisis Homogénea Enantioselectiva), Generalitat de Catalunya (2009SGR0259) and the ICIQ foundation for financial support. A. S. and R. R. acknowledge MINECO for predoctoral fellowships. S. D.–G. acknowledges MINECO for a "Torres Quevedo" contract.

**Notes and references**

1 (*a*) P. R. Schreiner, *Chem. Soc. Rev*. 2003, **32**, 289-296; (*b*) P. M. Pihko, *Angew. Chem. Int. Ed.* 2004, **43**, 2062-2064; (*c*) J. Seayad and B. List, *Org. Biomol. Chem.* 2005, **3**, 719-724; (*d*) Y. Takemoto, *Org. Biomol. Chem.* 2005, **3**, 4299-4306; (*e*) T. Akiyama, J. Itoh and K. Fuchibe, *Adv. Synth. Catal.* 2006, **348**, 999-1010; (*f*) S. J. Connon, *Chem. Eur. J.* 2006, **12**, 5418-5427; (*g*) M. S. Taylor and E. N. Jacobsen, *Angew. Chem. Int. Ed.* 2006, **45**, 1520-1543; (*h*) S. J. Connon, *Angew. Chem. Int. Ed.* 2006, **45**, 3909-3912; (*i*) A. G. Doyle and E. N. Jacobsen, *Chem. Rev*. 2007, **107**, 5713-5743; (*j*) T. Akiyama, *Chem. Rev*. 2007, **107**, 5744-5758; (*k*) A. Dondoni and A. Massi, *Angew. Chem. Int. Ed.* 2008, **47**, 4638-4660; (*l*) M. Terada, *Chem. Commun*. 2008, 4097-4112; (*m*) X. Yu and W. Wang, *Chem. Asian. J.* 2008, **3**, 516-532; (*n*) H. Miyabe and Y. Takemoto, *Bull. Chem. Soc. Jpn*. 2008, **81**, 785-795; (*o*) Z. Zhang and P. Schreiner, *Chem. Soc. Rev*. 2009, **38**, 1187-1198; (*p*) J. N. Johnston, H. Muchalski and T. L. Troyer, *Angew. Chem. Int. Ed*. 2010, **49**, 2290-2298; (*q*) M. Terada, *Bull. Chem. Soc. Jpn*. 2010, **83**, 101-119; (*r*) G. W. Amarante, M. Benassi, H. M. S. Milagre, A. A. C. Braga, F. Maseras, M. N. Eberlin and F. Coelho, *Chem. Eur. J.* 2009, **15**, 12460-12469; (*s*) M. Terada, *Synthesis* 2010, 1929-1982; (*t*) N. Kumagai and M. Shibasaki, *Angew. Chem. Int. Ed*. 2011, **50**, 4760-4772; (*u*) M. Rueping, B. J. Nachtsheim, W. Ieawsuwan and I. Atodiresei, *Angew. Chem. Int. Ed*. 2011, **50**, 6706-6720; (*v*) J. Yu, F. Shi and L.-Z. Gong, *Acc. Chem. Res.* 2011, **44**, 1156-1171; (w) M. Rueping, A. Kuenkel and I. Atodiresei, *Chem. Soc. Rev*. 2011, **40**, 4539-4549; (*x*) K. Brak and E. N. Jacobsen, *Angew. Chem. Int. Ed*. 2013, **52**, 534-561.

2 (*a*) H. Ishibashi, K. Ishihara and H. Yamamoto, *Chem. Rec.* 2002, **2**, 177-188; (*b*) K. Ishihara, D. Nakashima, Y. Hiraiwa and H. Yamamoto, *J. Am. Chem. Soc*. 2003, **125**, 24-25; (*c*) H. Yamamoto and K. Futatsugi, *Angew. Chem. Int. Ed.* 2005, **44**,

1924-1942: (*d*) C. H. Cheon, T. Imahori and H. Yamamoto, *Chem. Commun*. 2010, **46**, 6980-6982.

3 C. H. Cheon, O. Kanno and F. D. Toste, *J. Am. Chem. Soc*. 2011, **133**, 13248-13251.

4 J. Díez, J. Gimeno, A. Lledós, F. J. Suárez and C. Vicent, *ACS Catal*. 2012, **2**, 2087-2099.

5 D. Carmona, M. P. Lamata, F. Viguri, R. Rodríguez, L. A. Oro, F. J. Lahoz, A. I. Balana, T. Tejero and P. Merino, *J. Am. Chem. Soc.* 2005, **127**, 13386-13398.

6 (*a*) J. F. Blake and W. L. Jorgensen, *J. Am. Chem. Soc*. 1991, **113**, 7430-7432; (*b*) J. F. Blake, D. Lim and W. L. Jorgensen, *J. Org. Chem*. 1994, **59**, 803-805.

7 D. L. Severance and W. L. Jorgensen, *J. Am. Chem. Soc.* 1992, **114**, 10966-10968.

8 M. Gruttadauria, F. Giacalone and R. Noto, *Adv. Synth. Catal*. 2009, **351**, 33-57 and references therein.

9 G. A. Olah, R. Krishnamurty and G. K. S. Prakash, In *Comprehensive Organic Synthesis*, Vol. 3 (Eds: B. M. Trost and I. Fleming), Pergamon Press, Oxford, 1991, pp. 293-339.

10 (*a*) K. A. Jørgensen, *Synthesis* 2003, 1117-1125; (*b*) M. Bandini, A. Melloni and A. Umani–Ronchi, *Angew. Chem. Int. Ed*. 2004, **43**, 550-556; (*c*) M. Bandini, A. Melloni, S. Tommasi and A. Umani–Ronchi, *SYNLETT* 2005, 1199-1222; (*d*) M. Bandini, A. Eichholzer and A. Umani–Ronchi, *Mini–Rev. Org. Chem.* 2007, **4**, 115-124; (*e*) T. B. Poulsen and K. A. Jørgensen, *Chem. Rev*. 2008, **108**, 2903-2915; (*f*) E. Marqués–López, A. Díez–Martínez, P. Merino and R. P. Herrera, *Curr. Org. Chem*. 2009, **13**, 1585-1609; (*g*) S.-L. You, Q. Cai and M. Zeng, *Chem. Soc. Rev*. 2009, **38**, 2190-2201; (*h*) M. Bandini and A. Eichholzer, *Angew. Chem. Int. Ed*. 2009, **48**, 9608-9644; (*i*) *Catalytic Asymmetric Friedel–Crafts Alkylations*; M.

Bandini and A. Umani–Ronchi, Eds.; VCH: Weinheim, Germany, 2009. (*j*) G. Bartoli, G. Bencivenni and R. Dalpozzo, *Chem. Soc. Rev*. 2010, **39**, 4449-4465. (*k*) M. Zeng and S.-L. You, *Synlett* 2010, 1289-1301.

11 W. Zhuang, N. Gathergood, R. G. Hazell and K. A. Jørgensen, *J. Org. Chem.* 2001, **66**, 1009-1013.

12 M. P. A. Lyle, N. D. Draper and P. D. Wilson, *Org. Lett.* 2005, **7**, 901-904.

13 S. Nakamura, K. Hyodo, Y. Nakamura, N. Shibata and T. Toru, *Adv. Synth. Catal.* 2008, **350**, 1443-1448.

14 C. Wolf and P. Zhang, *Adv. Synth. Catal.* 2011, **353**, 760-766.

15 Y. Hui, W. Chen, W. Wang, J. Jiang, Y. Cai, L. Lin and X. Liu, *Adv. Synth.Catal*. 2010, **352**, 3174-3178.

16 G. Grach, A. Dinut, S. Marque, J. Marrot, R. Gil and D. Prim, *Org. Biomol. Chem.* 2011, **9**, 497-503.

17 (*a*) B. Török, M. Abid, G. London, J. Esquibel, M. Török, S. C. Mhadgut, P. Yan and G. K. S. Prakash, *Angew. Chem. Int. Ed*. 2005, **44**, 3086-3089; (*b*) X. Han, B. Liu, H.-B. Zhou and C. Dong, *Tetrahedron: Asymmetry* 2012, **23**, 1332-1337.

18 W. Zhuang, T. B. Poulsen and K. A. Jørgensen, *Org. Biomol. Chem.* 2005, **3**, 3284-3289.

19 (*a*) W. Kashikura, J. Itoh, K. Mori and T. Akiyama, *Chem. Asian J*. 2010, **5**, 470-472; (*b*) J. Nie, G.-W. Zhang, L. Wang, Y. Zheng and J.-A. Ma, *Eur. J. Org. Chem*. 2009, 3145-3149.

20 M. Rueping, T. Bootwicha, S. Kambutong and E. Sugiono, *Chem. Asian J*. 2012, **7**, 1195-1198.

21 Complex **1** crystallises with one additional molecule of water.[4] Free water has to be excluded from the solution to avoid the formation of ethyl 3,3,3–trifluoropyruvate

hydrate: B. Dolenský, J. Kvícala, J. Palecek and O. Paleta, *J. Fluorine Chem.* 2002, **115**, 67-74.

22 D. Balcells and F. Maseras, *New J. Chem*. 2007, **31**, 333-343.

23 T. Fjermestad, M. A. Pericàs and F. Maseras, *Chem. Eur. J*. 2011, **17**, 10050-10057.

24 H. Fernández–Pérez, S. M. A. Donald, I. J. Munslow, J. Benet–Buchholz, F. Maseras and A. Vidal–Ferrán, *Chem. Eur. J*. 2010, **16**, 6495-6508.

25 D. Carmona, C. Cativiela, R. García–Correas, F. J. Lahoz, M. P. Lamata, J. A. López, M. P. López–Ram de Víu, L. A. Oro, E. San José, F. Viguri, *Chem. Commun*. 1996, 1247-1248.

26 For the preparation of the ruthenium complex **6**: D. Carmona, M. P. Lamata, F. Viguri, J. Ferrer, N. García, F. J. Lahoz, M. L. Martín and L. A. Oro, *Eur. J. Inorg. Chem.* 2006, 3155-3166. The diastereomeric mixture of the osmium complex **7** was similarly prepared.

27 M. J. Frisch, G. W. Trucks, H. B. Schlegel, G. E. Scuseria, M. A. Robb, J. R. Cheeseman, J. A. Montgomery, Jr., T. Vreven, K. N. Kudin, J. C. Burant, J. M. Millam, S. S. Iyengar, J. Tomasi, V. Barone, B. Mennucci, M. Cossi, G. Scalmani, N. Rega, G. A. Petersson, H. Nakatsuji, M. Hada, M. Ehara, K. Toyota, R. Fukuda, J. Hasegawa, M. Ishida, T. Nakajima, Y. Honda, O. Kitao, H. Nakai, M. Klene, X. Li, J. E. Knox, H. P. Hratchian, J. B. Cross, C. Adamo, J. Jaramillo, R. Gomperts, R. E. Stratmann, O.Yazyev, A. J. Austin, R. Cammi, C. Pomelli, J. W. Ochterski, P. Y. Ayala, K. Morokuma, G. A. Voth, P. Salvador, J. J. Dannenberg, V. G. Zakrzewski, S. Dapprich, A. D. Daniels, M. C. Strain, O. Farkas, D. K. Malick, A. D. Rabuck, K. Raghavachari, J. B. Foresman, J. V. Ortiz, Q. Cui, A. G. Baboul, S. Clifford, J. Cioslowski, B. B. Stefanov, G. Liu, A. Liashenko, P. Piskorz, I.

Komaromi, R. L. Martin and D. J. Fox, Gaussian, Inc., Wallingford CT, 2009. Gaussian 09, Revision A.02.

28 Y. Zhao and D. G. Truhlar, *Theor. Chem. Acc.* 2008, **120**, 215-241.

29 (*a*) P. Fuentealba, H. Preuss, H. Stoll and L. v. Szentpaly, *Chem. Phys. Lett*. 1982, **89**, 418-422; (*b*) M. Dolg, U. Wedig, H. Stoll and H. Preuss, *J. Chem. Phys*. 1987, **86**, 866-872; (*c*) G. Igel-Mann, H. Stoll and H. Preuss, *Mol. Phys*. 1988, **65**, 1321-1328; (*d*) D. Andrae, U. Haeussermann, M. Dolg, H. Stoll and H. Preuss, *Theor. Chem. Acc*. 1990, **77**, 123-141.

30 (*a*) W. J. Hehre, R. Ditchfield and J. A. Pople, *J. Chem. Phys*. 1972, **56**, 2257–2261. (*b*) G. A. Petersson, A. Bennett, T. G. Tensfeldt, M. A. Al-Laham, W. A. Shirley and J. Mantzaris, *J. Chem. Phys*. 1988, **89**, 2193-2218.

31 A. V. Marenich, C. J. Cramer and D. G. Truhlar, *J. Phys. Chem. B* 2009, **113**, 6378-6396.

**Graphical contents entry**

**Chiral Transition–Metal Complexes as Brønsted–Acid Catalysts for the Asymmetric Friedel–Crafts Hydroxyalkylation of Indoles**

Daniel Carmona,* M. Pilar Lamata, Antonio Sánchez, Fernando Viguri, Ricardo Rodríguez, Luis A. Oro, Chunhui Liu, Silvia Díez–González, and Feliu Maseras*

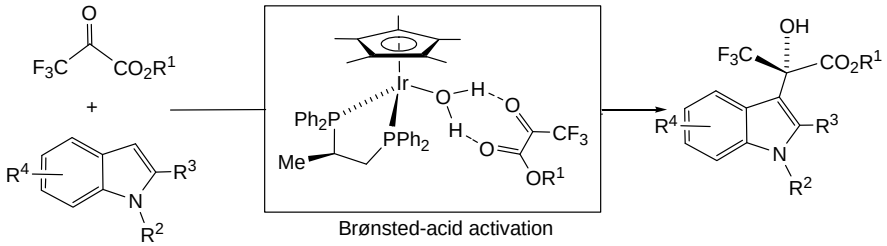


Water is the catalyst! The transition metal complex "only" modulates its acidity and provides a chiral environment.